Noise Produced By Cavitation From Various Cavitating Sources

الضوضاء المنبعثة من التكهف من مصادر مختلفة للتكهف

M.A. Hosien and S.M. Selim

Mechanical Power Engineering Department, Faculty of Engineering, Menoufyia University, Shebin El-Kom Egypt

الملخص

لقد تم فى هذه الدراسة اجراء قياسات الضغط الصوتى لخمس اشكال مختلفة وهم الشكل المثلثى ,الاسطوانة الدائرية, الشكل ذو الخطوة الخلفية، الشكل ذو الخطوة الامامية، والشكل المثلثى المتماثل 60^0 .ولكل شكل من الاشكال تمت الاختبارات على حجمان 20mm, 10 mm. وقد تم تسجيل spectrograms فى 1/3 octave band. وقد اجريت الاختبارات فى مدى واسع لسرعات السريان ومعاملات التكهف لمعرفة تاثيركل منها على الضوضاء الناجمةعن التكهف. وقد اظهرت النتائج للاشكال المختلفة انه عند ثبوت السرعة لا توجد علاقة واضحة بين مستوى الضغط الصوتى ومعامل التكهف. الاتجاه العام يبين ان مستوى الضغط الصوتى يزيد مع نقص معامل التكهف حتى يصل الى أعلى قيمة لة ثم يقل مرة اخرى. بينت النتائج ايضا ان مستوى الضغط الصوتى يعتمد بشدة على سرعة السريان للاشكال الخمسة. عند قيم ثابتة لمعامل التكهف ولكل شكل يوجد علاقة اسية واضحة بين مستوى الضغط السمعى و السرعة. وقد تبين ان اس السرعة يتغير كثيرا مع كل من شكل مصدر التكهف وقيمة معامل التكهف ,الا انة لا يعتمد على حجم مصدر التكهف الا للشكل المثلثى المتماثل. فعلى سبيل المثال عند تغير السرعات فى مدى 20-40 m/s وللشكل المثلثى المتماثل 60^0 فان قيمة أس السرعة يتراوح ما بين (2.3-6.2) معتمدا على معامل التكهف . فى مدى واسع يؤيد اس السرعة النتائج النظرية والتى تبين ان مستوى الضغط الصوتى يتغير مع السرعة U^4 عند ثبوت معامل التكهف.

Abstract

In the present study the sound pressure measurements were obtained for five configurations, con. –div. wedge, circular cylinder, rear facing step, forward facing step and 60° symmetric wedge. For each configuration two sizes, 10 mm and 20 mm, were used. Spectrograms were recorded with a 1/3 octave band. A wide range of velocities and cavitation numbers were tested to observe its effect upon the noise.

The results indicated that for all tested configurations, at constant flow velocity there was no clear relationship between the sound pressure level and cavitation number. The general trend was the sound pressure level increased as the cavitation number decreased reaching abroad peak and then decreased again. The sound pressure level was found to be strongly dependent on the flow velocity for the five configurations. For each configuration at fixed values of cavitation number there was a clear power relation between SPL and the flow velocity. The velocity exponent varied widely with both the cavitation number and cavitation source configurations, although not with cavitation source size. For instance, it is found that, for velocities ranging from 20-40 m / sec and constant cavitation source for 20 mm 6^0 symmetric wedge, the velocity exponent ranged from 2.3 to 6.2 depending on the cavitation number. The magnitude of the sound pressure level might be independent of the size of the cavitation source for all configurations tested except the con.-div. wedge. The velocity exponent for the broad band width was found to confirm the present theoretical results which indicate that the sound pressure level various at U^4 at constant cavitation number.

Key words: Cavitation, noise, sounds pressure level.

1. Introduction

It is well known that cavitation in hydraulic machines is always associated with noise phenomena. Since cavitation noise is produced by the collapse of cavitation bubbles it would seem reasonable that some relationship exists between the intensity of the cavitation noise and the cavitation conditions (i.e. cavitation number and flow velocity). Cavitation noise has been used as an easily detectable and measurable phenomenon for determining the onset of cavitation in hydraulic devices. It has also been used in evaluating the possibility of damage.

Many investigators have found the inception of cavitation indicated by the rapid increase of noise during tests in water tunnels [1-4] pumps [5-15], water turbines and propellers [16-19].

Received: 20 October, 2015 – Accepted: 30 November, 2015

Yan et al. [20] proposed a novel method to detect cavitation based on active ultrasonic flow field velocity measurement. The theory of ultrasonic modulation by fluid motion was analyzed. The ultrasonic propagating in a flow field was modulated by the transient fluid velocity information. The continuous demodulation of the received signal enabled the measurement of the flow field velocity pulsation. The relationship between the demodulated signal and the velocity spatial mean value, which is the particle velocity component in the direction of the ultrasonic signal along the path of ultrasonic propagation, was established. The modulating signal was recovered by following baseband signal processing.

For cavitating flows the dependence of noise upon flow velocity had been little studied in the past and the relationship between noise and cavitating source size and shape has not yet been established. It has been shown by many investigators that the noise level should increase exponentially with the flow velocity. In the analysis reported by Fitzpatrick and Strasberg [21], it has been shown that the velocity exponent value for cavitation behind a cylinder is 4. Blake et al. [22] found experimentally the value of the velocity exponent for flow past a hydrofoil to be in the range of 3 to 4. Varga [23] reported that the velocity exponent is 5. Barker [24] has stated that the value of the exponent varies from 6 at the low frequency end of the noise spectrum (<1 kHz) to 10 at the high frequency end of the noise spectrum (10 kHz - 100 kHz) for flow past a cavitating hydrofoil. For cavitation tests behind a circular cylinder, King [25] measured the maximum sound pressure level in a 40 kHz band. King [25] results indicated that the velocity exponent is 6.25.

Hence, the aim of the present work is to investigate the dependence of the noise level upon flow velocity, cavitation number and cavitation source shape and size.

2. Cavitation Noise

A collapsing cavity in a liquid produces a volume pulsation which may be regarded as an acoustic monopole. An estimate of the source strength may be made by considering the pressure and velocity produced by a collapsing empty spherical cavity. This problem was first investigated in detail by Rayleigh (1917) and he derived an expression for the pressure perturbation in the liquid, which predicts that the pressure increases indefinitely as the cavity collapses to zero radiuses. In reality, the collapse will be arrested at a small but finite radius with gas and vapour trapped in the cavity. Although the result was derived for an incompressible liquid, it can be used to predict the sound pressure provided the sound wavelength is very much greater than the cavity size. The acoustic energy radiated from the collapsing cavity can be calculated by integrating the square of the pressure perturbation over the time for the cavity to collapse. Unfortunately the integral does not converge as the cavity radius tends to zero, and it may assumed that the collapses arrested at a small radius which is always the same fraction of the maximum cavity radius. This is equivalent to assuming that the pressure of dissolved gas relative to the ambient pressure is always a constant. Therefore, we can derive a scaling law for the sound energy released in terms of collapse pressure Δp and maximum cavity radius R_m. Growing and collapsing cavitation bubbles produce volume pulsations in the liquid which are equivalent to a distribution of acoustic monopoles. The sound pressure field, p, produced by a pulsating spherical cavity is given by:

$$P = \frac{\rho \ddot{V}}{4\pi r} = \rho\left(R\ddot{R} + 2\dot{R}^2\right)\frac{R}{r} \qquad (1)$$

Where V: is the instantaneous volume of the cavity and R its radius. The distance between source and observer is r. Using Rayleigh's analysis of a collapsing spherical cavity, the cavity wall velocity, $\dot{R}$, can be calculated and t_c is the time taken for the bubble to collapse from its maximum size R_m to zero radius. Rayleigh's results are:

$$\dot{R}^2 = \frac{2}{3}\frac{\Delta P}{\rho}\left[\frac{R_m^3}{R^3} - 1\right] \qquad (2)$$

$$t_c = R_m\sqrt{\frac{\rho}{\Delta P}} \quad (3)$$

Where Δp: is the pressure difference between the liquid and the cavity.
By using equation (2), it may be deduced from equation (1) that the sound pressure is given by:

$$P = \frac{1}{3}\Delta P\left[\frac{R_m^3}{R^3} - 4\right]\frac{R}{r} \sim \Delta P\frac{R_m^3}{R^2 r} \quad (4)$$

The approximate from of equation (4) applies as the bubble collapses to zero radius and indicates that the pressure rises to infinite limit at the point of collapse. The mean square pressure of the radiation is given by:

$$\overline{P}^2 = \nu\int_{-\infty}^{\infty} P^2\, dt \quad (5)$$

Where ν: is the number of bubbles collapsing in unit time or in the case of the cycling flow the frequency of repetition. This integral becomes indefinitely large as the bubble approaches zero size but in reality the collapse is arrested by gas trapped in the cavity at a small but finite value of R. It is reasonable to assume that this value of R is always the same fraction of the maximum bubble size, R_m. Hence using equation (4) and the result that the time scale is given by equation (3), from equation (5) the mean square pressure scales may be estimated according to:

$$\overline{P}^2 \sim \nu\rho^2\left[\frac{\Delta P}{\rho}\right]^{3/2}\frac{R_m^3}{r^2} \quad (6)$$

By assuming that ν scaled as t_c^{-1}, equation (6), has been derived that the cavitating sources are in a free field. This condition is approximately satisfied at low values of σ, when the effective sound speed is reduced by the presence of vapour bubbles. The sound wavelengths will be correspondingly reduced, thus allowing a large number of modes to propagate. In this condition the cavitating sources are effectively in a free field. Applying equation (6) to the cavitating sources, for which it is known that the cavity grows from the throat and is ultimately shed when a jet of liquid has penetrated upstream underneath the cavity. The cavity is convicted downstream and then collapse in the region of higher pressure downstream of the source throat.

This process is approximately periodic and the frequency is proportional to U/λ. The pressure in the reattachment region will approach the stagnation pressure and since the ambient pressure in the throat is virtually the vapour pressure, the stagnation pressure will be equal to $P_v + \frac{1}{2}\rho U^2$. Consequently the pressure difference collapsing the bubbles will be of order $\frac{1}{2}\rho U^2$.

Assuming that, the bubble size, R_m, will be proportional to the cavity, λ. In the present noise experiments, the pressure transducer was flush mounted in the working test section of the water tunnel at a fixed distance downstream of the throat of the cavitating source, i.e., r is considered constant. Hence, on substituting these assumptions into equation (6) the following is obtained:

$$\overline{P}^2 \sim \rho^2 U^4 \lambda^2 \quad (7)$$

The experimental results indicated that the variation of cavity length, λ, for various cavitation sources as a function of cavitation number follow a simple power law $\lambda\ \alpha\ \sigma^n$ for the cavitation sources. The cavitation number index varies with the cavitation source geometry (e.g., -0.1 for con-div wedge, -0.27 for rear-facing step, -0.3 for forward –facing step, -0.574 for circular cylinder and -0.785 for 60^0 symmetrical wedge). Therefore, using these results in equation (7) the sound pressure scales as given in table 1.

Table1. Sound pressure scales for various cavitation sources.

Cavitation source geometry	$\overline{P}^2$ (Sound pressure)	Cavity length exponent (n)
Con.-div.	$\rho^2 U^4 \sigma^{-2}$	-1
Circular cylinder	$\rho^2 U^4 \sigma^{-1.148}$	-0.574
60^0 symmetrical wedge	$\rho^2 U^4 \sigma^{-1.57}$	-0.785
Rear-facing step	$\rho^2 U^4 \sigma^{-0.54}$	-0.27
Forward-facing step	$\rho^2 U^4 \sigma^{-0.6}$	-0.3

3. Measurement Technique

Measurements of pressure produced by cavitation have been obtained by a Vibrometer quartz electric transducer (type 6 QP 500) of diameter 6 mm which was flush mounted in the working section of the tunnel. It was placed about 215 mm. and 130 mm downstream from the throat of the cavitation source for the large and small working sections of a closed circuit water tunnel, respectively. The transducer was connected to a charge amplifier type (TA-3/c). The RMS voltage output from the charge amplifier was measured using a "Bruel and Kjaer" precision sound level meter (type 2203).

The output signal of the charge amplifier was analyzed using two methods. The main measurement made was the sound pressure level with reference to 1μ bar over frequency bandwidth of about 31.5 Hz to 31.5 kHz. Measurements of the 1/3 octave band spectrum were also made using a "Bruel and Kjaer" 1/3 octave frequency analyzer (type 2112) which is connected to the B and K level recorder type 2305. Using this system a noise signal can be analyzed and a spectrogram giving the sound pressure level of each 1/3 octave band from 25 Hz to 40 kHz obtained.

The sound pressure level and the spectrograms were obtained for five cavitation source configurations, namely con.-div. wedge, rear facing step, circular cylinder, 60^o symmetric wedge and forward facing step. For each configuration two sizes, 10 mm and 20 mm are used. Details of the configurations are given in Fig. 1. The experimental program was conducted in a 40 x 20 mm working section of the water tunnel. Details of the experimental setup are in [26].

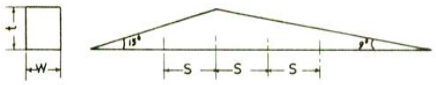

t	w	s
20	20	30
10	10	15

Details of con. - div. wedge sources.

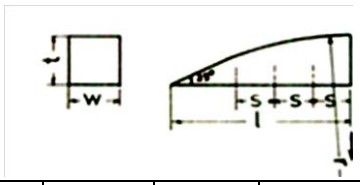

t	w	s	r	l
20	20	15	100	72
10	10	75	65	36

Details of rear- facing step sources.

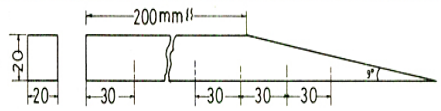

Details of forward- facing step ources.

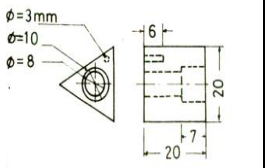

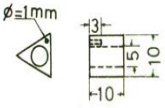

Details of 60^0 symmetrical wedge sources

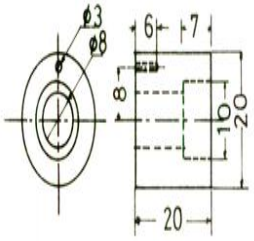

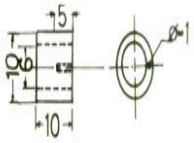

Details of circular cylinder sources.

Fig. 1 Details of cavitating sources (Dim. mm)

4. Experimental Results and Discussion

4.1 Effect of Cavitation Number on Sound Pressure Level at Constant Flow Velocity

4. 1.1 Rear and Forward Facing steps Sources

The exact variation of the sound pressure level (SPL) with σ at a constant flow velocity of 28 m/s is shown in Fig.2. In general this Figure shows that the sound becomes detectable at approximately σ = 0.4. The SPL increases rapidly with decreasing the cavitation number (σ) in the region between σ = 0.4 and 0.11 for rear facing step and between σ =0.45 and 0.11 for forward facing step. In these regions the cavitation bubbles appeared within the shear zone. Below σ = 0.11 there is a sudden rise in the sound pressure level. This should represent the starting point of large bubble cavitation. In the region between σ =0. 11 and 0.055 for rear facing step and σ = 0.11 and 0.068 for forward facing step, if the cavitation number decreases the SPL increases, also in this region does not appear to follow a simple power law.

At values of σ less than 0.055 for rear facing step and 0.068 for forward facing step, there is a tendency for the SPL to decrease as σ decreases. A possible explanation for this is that below these values the longitudinal fluctuations of the downstream end of the cavity become most pronounced. This amounts to a reduced sound pressure level at lower cavitation numbers.

A comparison of SPL between 10 mm and 20 mm sources, Fig. 2, shows that the variation of SPL with σ is the same for the two sources at a given configuration, except for the anomalous region below σ = 0.05. This means that the SPL is almost independent of source size for similar flow with rear and forward facing steps for σ ≤ 0.05. This trend is in full agreement with the present simple theoretical considerations.

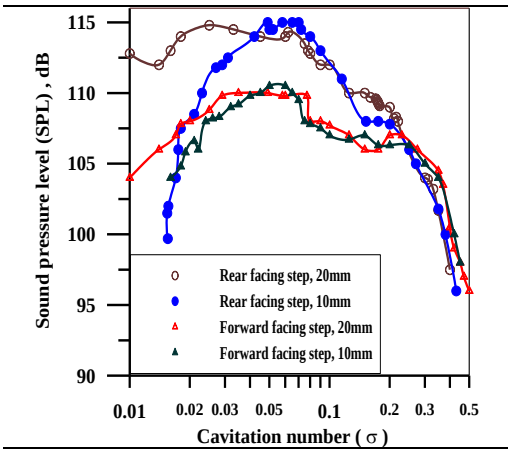

Fig.2 Variation of sound pressure level with cavitation number for rear facing step and forward facing step at a flow velocity of 28 m / s.

4.1.2. Con.-div. Wedge Source

The variation of SPL with cavitation number (σ) is given in Fig.3 for 20 mm and 10 mm con.-div. wedges at fixed flow velocities. Fig.3 indicates that the SPL becomes detectable at σ = 0.2 for 20 mm source and σ = 0.18 for the 10 mm source. This should be the starting point of the formation of a fixed vapor cavity attached to the surface of the source and consists of large cavities.

As the cavitation number (σ) is decreased, more bubbles are produced and the extent of cavitation increases rapidly with higher bubble collapse pressure which in turn increases the radiated sound pressure level, as shown in Fig.3. Moreover this figure shows that the sound pressure level increases rapidly with decreasing σ obeying a power law of about $\sigma^{-2.2}$ in the region between σ = 0.16 and 0.03 for the 20 mm source and $\sigma^{-3.5}$ in a similar range of σ the 10 mm source. The values of the cavitation number exponent at different velocities are almost the same. The cavitation number exponent is larger than that the predicted by theoretical consideration. For further reduction in σ towards the breakdown condition, the sound pressure level reduces very rapidly. At values of σ < 0.025, there is a tendency for the sound pressure level to decrease as σ decreases, as shown in Fig 3, and this may be attributed to the following factors: (l) at lower cavitation numbers the

cavitation zone extends rapidly and the dominant bubbles size becomes larger and as the bubbles grow they absorb more and radiate less noise; (2) also at lower cavitation numbers, the re-entrant jet loses its momentum before reaching the cavity surface, therefore the cavity shedding frequency becomes less definite, resulting is less noise, (3) below; $\sigma = 0.025$, there is a rapid increase in the distance between the center of the cavity collapse and the transducer and therefore conditions are quieter. Consequently, the overall noise of the bubbles will decrease with σ. A comparison of SPL between 20 mm and 10 mm con-div wedges at fixed flow velocities, Fig 3, shows that on average the measurements for the 20 mm source are about 6-14 dB reference 1 μ bar higher for $\sigma > 0.03$ and about 4-6 dB ref. 1 μ bar higher for $\sigma < 0.03$ than for the 10 mm source. This means that for con-div wedges the SPL is dependent on the size of the source. This is somewhat contrary to the present theoretical analysis.

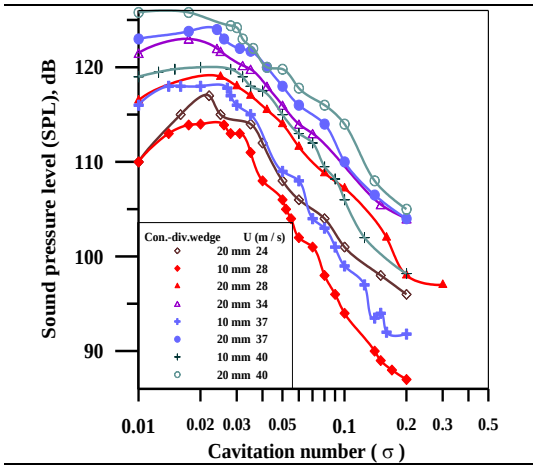

Fig. 3 Variation of sound pressure level with cavitation number for con.-div. wedge at fixed velocities.

4.1.3 Circular Cylinder and 60^0 Symmetric Wedge Sources

Figs. 4 and 5 show the SPL as a function of cavitation number for circular cylinders and 60^o symmetric wedges, respectively, at constant flow velocities. Due to the rig pressure limitation, the noise data for the higher velocities could not be obtained for the higher cavitation numbers. Nevertheless the cavitation number for the peak noise can be identified for all the velocities reported here. In general Figs 4 and 5 shows that the SPL does not appear.to follow a simple power law.

Figures 4 and 5 indicate that the SPL maintained nearly a constant value from the inception condition down to a lower critical cavitation number at which the SPL rises suddenly. This sudden rise takes place within a range of σ values about 0.05 wide for circular cylinders and 0.07 for 60^o symmetric wedges. The sudden rise in the SPL should be the starting point of the large cavitation bubbles which occur in the two vortex regions being shed behind the cavitation source. In addition this sudden rise in the SPL could be easily detected by ear and was coincident with the development of two lines of bubbles being alternately shed from both sides of the source with each line having a characteristic bubble rotation direction.

With a reduction in σ the SPL increases steadily, reaching a maximum value and decreasing with further reduction of the cavitation number, as shown in Figs 4 and 5. At the lower values of σ, at which the SPL falls off the clusters were not shed into two alternate rows but the separation frequencies of clusters become random and low. This amounts to a reduced SPL at low cavitation numbers.

Figures 4 and 5 show that the cavitation numbers at which the maximum SPL occurred depend strongly on the flow velocity for a given source. The values of σ at which SPL become maximum increase with decreasing flow velocity. This is possibly because at low velocities the effect of the tunnel walls is more significant than at high velocities.

It can be seen from Figure 4 that on average the sound pressure levels for the 20 mm cylinder are about 1-3 dB higher for $\sigma \leq 0.1$ than for the 10 mm cylinder. Figure 5 shows that the SPL for 20 mm 60^0 symmetric wedge is higher for the full range of σ reported ($0.01 < \sigma < 0.2$) than for the 10

mm source. Nevertheless, considering the difficulties involved in experimentally determining the SPL and the variation in tests conditions, the SPL for the two sizes might be almost the same. Hence, the SPL may be independent of the size of both circular cylinder and 60^0 symmetric wedge configurations at similar flow conditions. This trend is similar to that in the present model.

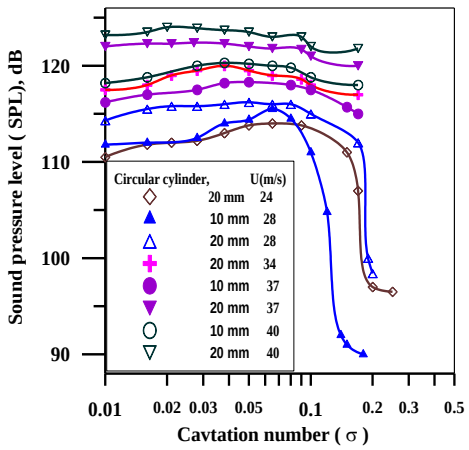

Fig.4 Variation of sound pressure level with cavitation number for circular cylinder at fixed velocities.

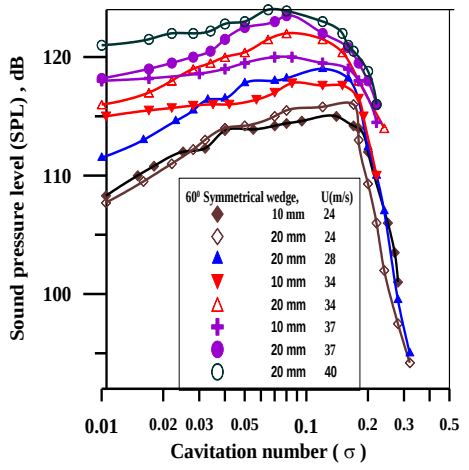

Fig.5 Variation of sound pressure level with cavitation number for 60^0 symmetrical wedge at fixed velocities.

4.2 Effect of Velocity on the Sound Pressure Level at Fixed Cavitation Numbers

The variation of SPL with velocity at different cavitation numbers is given in Figs 6-10 for 20 mm five sources with various configurations. These figures show that for all sources and a given cavitation number, as the velocity increases the SPL increases at some power of velocity. The reason for this variation of the SPL with velocity is not obvious. Nevertheless, it can be seen that the most important factors which contribute to the cavitation noise at constant cavitation number are the collapse pressure, collapse time, the number of the collapsing cavities and the critical nuclei size, which are mainly a function of velocity. The combination of these factors may cause an increase of SPL which is proportional to some power of flow velocity.

The experimental values of the velocity exponent (m) in this investigation showed that the velocity exponent depends strongly on the cavitation number with a possible variation between the limits of 2.3 and 6.73.The average of the velocity exponent is nearly 4.5 which is somewhat close to the exponent 4 which predicted by the present theoretical consideration.

Figure 11 shows the variation of the velocity exponent (m) with cavitation number for the 20 mm sources for a range of velocities from 24 m/sec to 40 m/sec. Generally, the figure shows that once the noise becomes detectable at a certain cavitation number with decreasing σ the velocity exponent does not very much, decreases, and reaches a minimum value, thereafter m increases towards the breakdown value for all the 20 mm sources except the 20 mm 60^0 symmetric wedge. For the 20 mm 60^0 symmetric wedge, the velocity exponent decreases with increasing σ, exhibits a constant value, decreases to a minimum as σ increases, then increases for higher values of σ. On the whole, the velocity exponent depends strongly on both the cavitation source configuration and cavitation number. This is mainly because for a given source at a range of cavitation numbers between 0.2 and 0.01 the cavity size varies widely, suggesting that different types of sound waves are generated by the collapse of the cavities in the working section with each type of sound wave likely

to have different scale law. The difference in exponent value between one configuration and another can be interpreted as a change in the type of cavitation as each source configuration produced different flow regimes. In addition to the change of the position of the center of cavity with respect to the fixed position of the transducer (i.e., r is not constant).

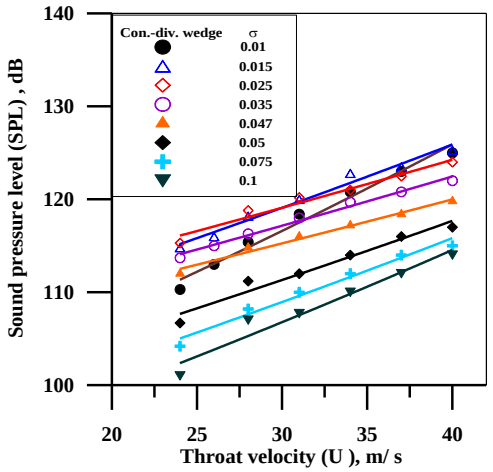

Fig.6 Variation of sound pressure level with flow velocity at fixed cavitation numbers for con.-div. wedge 20mm cavitating sources.

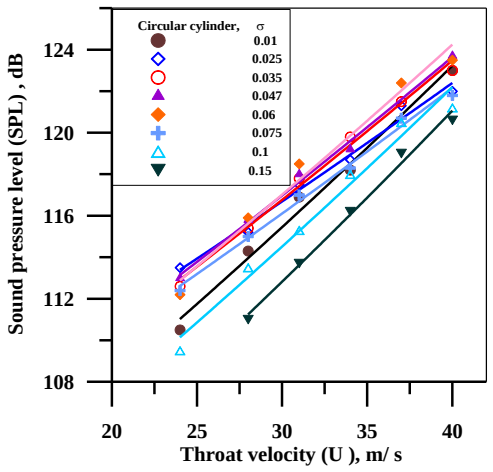

Fig.7 Variation of sound pressure level with flow velocity at fixed cavitation numbers for circular cylinder 20mm cavitating sources.

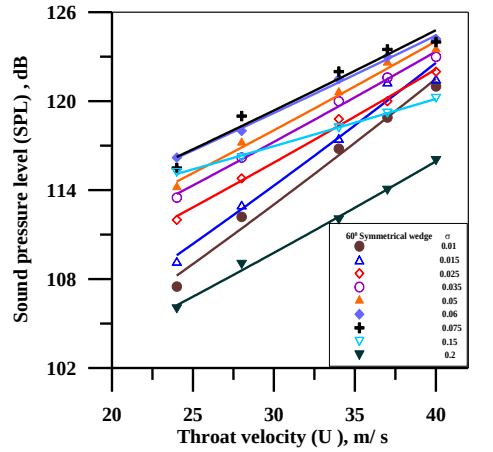

Fig.8 Variation of sound pressure level with flow velocity at fixed cavitation numbers for 60^0 symmetical wedge 20 mm cavitation sources.

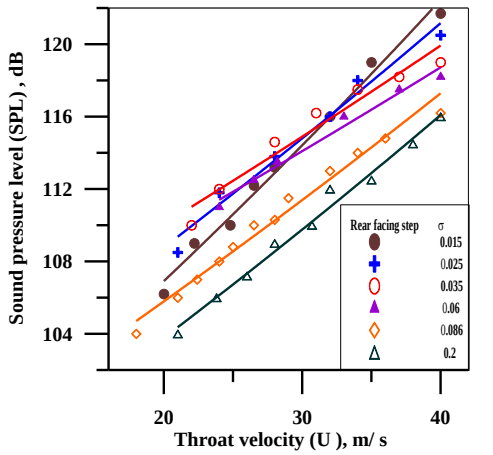

Fig.9 Variation of sound pressure level with flow velocity at fixed cavitation numbers for rear facing step 20mm cavitating sources.

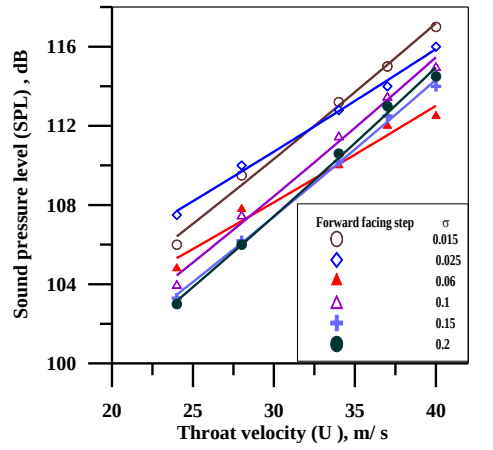

Fig.10 Variation of sound pressure level with flow velocity at fixed cavitation numbers for forward facing step 20mm cavitating sources.

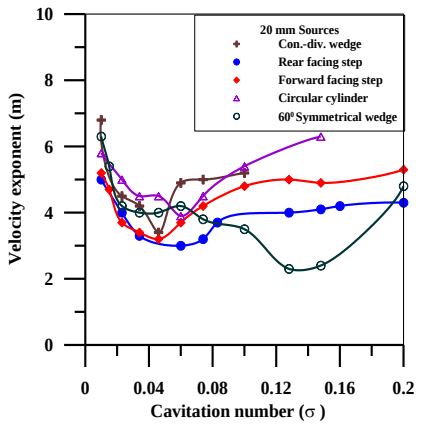

Fig.11 Velocity exponent (m) as a function of cavitation number for 20mm cavitating sources.

4.3 1/3 Octave Band Spectra

Typical 1/3 octave band spectra spectrograms, at fixed cavitation numbers of 0.035 and varied velocities are shown in Figures 12 and 13 for the 20 mm 60^0 symmetrical wedge 10 mm circular cylinder. Figs.12 and 13 shows that the spectra at different velocities are similar in shape although at different levels with two marked Peaks. In addition, Figs.12 and 13 indicate that the peak frequency increases slightly with increasing flow velocity. Figs. 14 and 15 show a typical 1/3 octave band spectra spectrograms at fixed flow velocity of 37 m/s and for three cavitation numbers for 20 mm 60^0 symmetric wedge and 20 mm con-div wedge. Figures 14 and 15 illustrate that the spectra at different cavitation numbers and similar in shape but have different levels with two marked peaks. In examining the corresponding results at all velocities between 22 and 40 m/sec for ten sources (not shown here) reveal that the spectra exhibit parallel stacking patterns from the frequencies between 1.35 kHz and 40 kHz. This leads to the conclusion that the spectrum energy in this range of frequencies can give a better indication of cavitation noise.

The experimental values of the velocity exponent, which were obtained from analyzing the spectral levels given by the 1/3 octave spectra spectrograms, are shown in Table 2. Table 2 indicates the velocity exponent at σ =0.035 in the frequency ranges 1.35 - 40 kHz, 1.35 - 8 kHz, 10 - 40 kHz, and broad band width frequencies (Fig .11). It can be seen that the value of the velocity exponent changes little over the different frequency ranges in the case of the 20 mm sources. However, in the case of 10 mm sources, although the velocity exponents for frequency ranges 1.35 - 40 and 1.35 - 8 kHz are almost the same for the same geometry, the exponent for the high frequencies between 10 kHz and 40 kHz roughly equals one and is independent of the source shape. In addition Table 2 indicates that the velocity exponent values for the three ranges of frequency are higher than for the broad bandwidth except the high range 10 - 40 kHz for 10 mm sources. The velocity exponent for the broad band with for all sources is very close to four which is predicted by the present theoretical analysis for cavitation noise.

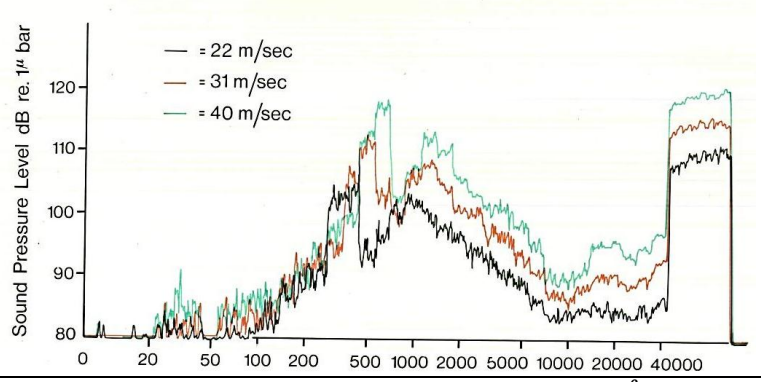

Fig. 12 Typical spectrograms of cavitation noise for the 20 mm 60^0 symmetrical wedge in the large tunnel at various flow velocities with σ = 0.035

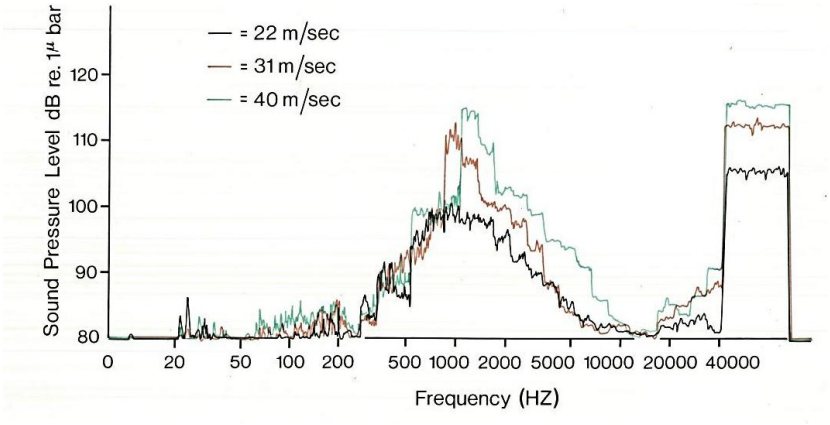

Fig. 13 Typical spectrograms of cavitation noise for the 10 mm circular cylinder in the large tunnel at various flow velocities with σ = 0.035.

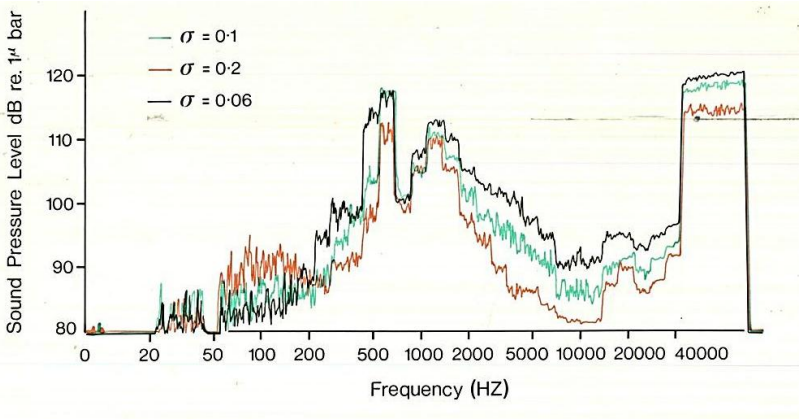

Fig. 14 Typical spectrograms of cavitation noise for the 20 mm 60^0 symmetrical wedge in the large tunnel at various cavitaion numbers with U = 37 m/s.

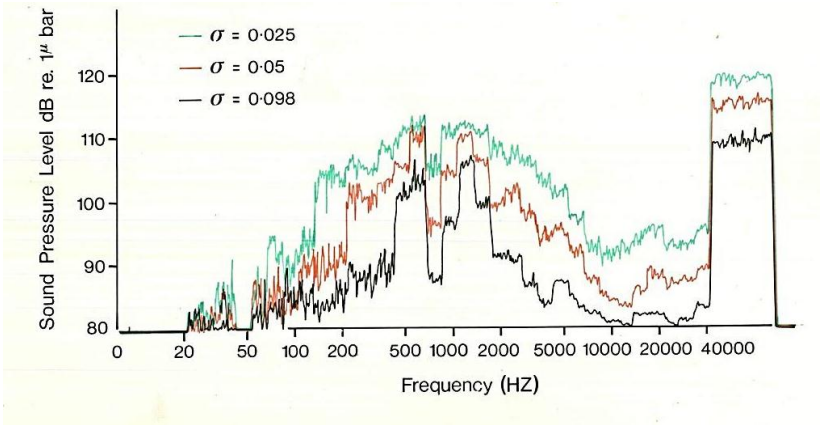

Fig. 15 Typical spectrograms of cavitation noise for the 20 mm con.-div. wedge in the large tunnel at various cavitaion numbers with U = 37 m/s.

Table 2: Velocity exponent for a range of velocities from 22 to 40 m/sec at different ranges of frequency and with σ = 0.035.

Cavitation source		Velocity Exponent (m)			
Shape	**size(mm)**	**1.35 -40KHz**	**1·35–8kHz**	**10-40kHz**	**Broad band width**
Circular cylinder	20	5 .26	5.26	5.26	4.47
	10	5	5	**1**	4.3
60^0 Symmetrical wedge	20	4.13	4.13	3.9	4.07
	10	4.2	4.2	**1**	3.9
Con.-div. wedge	20	5.31	5.31	5.1	4.23
	10	3	3	0.98	4.3
Rear facing step	20	4.3	4.3	4.28	3.35
	10	3.7	3.7	1.1	3.24
Forward facing step	20	4.6	4.58	4.6	3.5
	10	5.2	5.2	0.92	3.7

5. Conclusions

The conclusions, which can be drawn from this study, are:

1. At constant flow velocity there was no clear relationship between sound pressure level and cavitation number. The general trend was that the sound pressure level increased as the cavitation number decreased reached a broad peak and then decreased again.

2. The sound pressure level was found to be strongly dependent on the flow velocity. For each configuration at fixed values of cavitation numbers then was a clear power law relation. The values of the velocity power exponent varied widely with both the cavitation number and cavitation source.

3. The effect of flow velocity on the changes in spectral shapes were investigated for ten sources. The values of the velocity exponent at various ranges of frequency showed them to be almost the same for a given configuration and with $\sigma = 0.035$.

4. The velocity exponent for the broad band width was found to confirm the present theoretical results which indicate that the sound pressure level various at U^4 at constant cavitation number.

5. The sound pressure level might be independent of the size of the cavitation source for the all configurations tested in this investigation except for the con-div wedge, for this shape the sound pressure level was found to be dependent on the source size at fixed flow condition. The present theoretical analyses of cavitation noise confirm this relationship.

6. References

[1.] Il'Ichev V.I., and Kuznetsov, G.N., (1968), "Relationship between Acoustic Noise and Erosion in Hydrodynamic Cavitation", Soviet Physics Doklady, Vol. 13 No.4.

[2.] Deeprose, W.M., King, N.W., McNulty, P.J., and Pearsall, I.S., (1974), "Cavitation Noise, Flow Noise and Erosion", Cavitation Conf. IMech Engrs, Edinburgh.

[3.] Hutton, S.P. and Fry, S.A., (1983),"Correlation of Cavitation Noise and Erosion", Cavitation Conf. I Mech Engrs, Edinburgh.

[4.] Grant, M. and Lush, P.A., (1983),"The Measurements of Cavitation Noise in a Duct", Cavitation Conf. I Mech Engrs, Edinburgh.

[5.] Wolde, T.T., Moelker, W.H., and Mendte, K.W., (1974), "Experiences with Acoustical Methods for the

Detection of Cavitation in Pumps", Inst. Mech. Eng. Conf. on Cavitation.

[6.] Čudina, M., (2003)," Detection of Cavitation Phenomenon in a Centrifugal Pump Using Audible Sound", Mech. syst. signal process., Vol. 17, No. 6, 1335-1347.

[7.] Čudina, M., Prezelj, J., (2008)," Use of Audible Sound for Safe Operation of Kinetic Pumps", Int. j. mech. sci., Vol. 50, No. 9, 1335-1343.

[8.] McNulty, P. J. and Pearsall, I. S., (1982), "Cavitation Inception in Pumps", Journal of fluids engineering, March, Vol. 104, No. 3, 99-104.

[9.] Černetič, J., (2010)," Cavitation Detection in Centrifugal Pumps Using Sound and Vibration in Audible Range", Dissertation, Ljubljana.

[10.] Čudina ,M. , (2012), "Monitoring of Cavitation by Sound in Audible Range and Some New Proposals for Prevention Cavitation in Kinetic Pumps"5th Congress of Alps-Adria Acoustics Association, Petrčane, Croatia.

[11.] Černetič, J. and Čudina, M., (2012),"Cavitation Noise Phenomenon in Centrifugal Pumps ", 5th Congress of Alps-Adria Acoustics Association, 12-14 September, Petrčane, Croatia.

[12.] Černetič, J., (2009),"Use of Noise and Vibration Signals for Detection of Cavitation in Kinetic Pumps", Proc. IMechE, Part C: J. Mech. Eng. Sci., 223 (C7), 1645–1655.

[13.] Čudina, M., (2003)," Noise as an Indicator of Cavitation in a Centrifugal Pump", Acoust. phys., 49, 463-474.

[14.] Alfayez, L., Mba, D., and Dyson, G., (2005)," The Application of Acoustic Emission for Detecting Incipient Cavitation and the Best Efficiency Point of a 60KW Centrifugal Pump, Case Study", NDT & E International, Vol 38, no. 5, 354-358.

[15.] Alfayez, L., and Mba, D., (2005)," Detection of Incipient Cavitation and Determination of the Best Efficiency Point for Centrifugal Pumps Using Acoustic Emission", Journal of Mechanical Process Engineering, Part E, IMechE.

[16.] Beyer, J.R., and, Smith, T.G., (1982), "Acoustic Emission Characteristics of Model Frances Turbine Under Cavitating and Non-cavitating Conditions", International Symposium on Cavitation Noise, ASME, Arizona.

[17.] Sharma, S.D., Mani, K., and, Arakeri, V.H., (1990), "Cavitation noise studies on marine propellers", Journal of sound and vibration, 138(2), 255-283**.**

[18.] Bark, G., (1985),"Prediction of Propeller Cavitation Noise from Model Tests and its Comparison with Full Scale Data", Trans of the ASME, Jr of Fluid Eng., Vol.107 March.

[19.] Liu, S.Y. and Wang, S.Q., (2007), " Cavitation Monitoring and Diagnosis of Hydropower Turbine on Line Based on Vibration and Ultrasound Acoustic", Proceedings of the Sixth International Conference on Machine Learning and Cybernetics, Hong Kong, 5, 2976-2981.

[20.] Yan, Z., Liu, J., Chen, B., Cheng, X., and Yang, J., (2015), "Fluid Cavitation Detection Method with Phase Demodulation of Ultrasonic Signal", Applied Acoustics 87,198–204.

[21.] Fitzpatrick, H.M. and Strasberg, M., (1956), "Hydrodynamic Sources of Sound", 2nd Symp. Naval Hydro., Washington, D.C.

[22.] Blake, W. K., Wolpert, M.J., and Geib, F.E., (1977), "Cavitation Noise and Inception as Influenced by Boundary-Layer Development on a Hydrofoil", Journal of Fluid Mechanics, Vol. 80 No 4.

[23.] Varga, J.J., Sebestyen, G., and Fay, A., (1969),"Detection of Cavitation by Acoustic and Vibration Measurement Methods", La Houille Blanche, No.2.,

[24.] Barker, S.J., (1973), "Measurements of Radiated Noise from Cavitating

Hydrofoils", Cavitation and Polyphase Flow Forum, Atlanta.

[25.] King, N.U., (1973), "A Study of Cavitation Erosion and Noise in a Venturi Test Section", Fluid Mechanics Memo, No. A23, NEL, Glasgow.

[26.] Hosien, **M. A.** and Selim, S. M. , "A Study on Tip Clearance Vortex Cavitation Inception", Engineering Research Journal, Faculty of Engineering, Mataria-Cairo, Helwan University, Vol.122, June, 2009, M1-M25.

Nomenclature	
R_m	Maximum cavity radius
V	Instantaneous volume of the cavity
R	Cavity radius
$\dot{R}$	Cavity wall velocity
$\ddot{R}$	Cavity wall acceleration
R	Distance between source and observer
P	Sound pressure field
Δp	Pressure difference between the liquid and the cavity.
t_c	Time taken for the bubble to collapse
N	The number of bubbles collapsing in unit time
λ	Cavity length
$\bar{P}^2$	Sound pressure
U	Flow velocity
Σ	Cavitation number
P	Density